JOURNAL OF MATERIALS SCIENCE **32** (1997) 3013–3019

The role of boron in low-temperature synthesis of indialite (α-$Mg_2Al_4Si_5O_{18}$) by sol–gel process

T. SEI, K. ETO, T. TSUCHIYA
Department of Materials Science, Faculty of Industrial Science, Science University of Tokyo, Noda, Chiba 278, Japan

Powder and pellets composed mainly of indialite (α-$Mg_2Al_4Si_5O_{18}$) with 2.1 wt% added B_2O_3 were prepared by a sol–gel process using metal salts as raw materials. When heated at 900 °C for 6 h, the pellets showed a relative density of 91.4% of ideal cordierite (β-$Mg_2Al_4Si_5O_{18}$), a Vickers hardness of 1080 and a relative dielectric constant of 5.0 (at 1 MHz), which was the same value as that of cordierite. Magic angle spinning nuclear magnetic resonance measurements of ^{29}Si, ^{27}Al and ^{11}B showed that boron disturbed the formation of the Si–O–Al network below 300 °C and broke the network between 700 and 800 °C. The high homogeneity and fluidity caused by the melting helped indialite to crystallize directly from the amorphous state between 800 and 850 °C.

1. Introduction

Cordierite (β-$Mg_2Al_4Si_5O_{18}$) has a thermal expansion of $1.5 \times 10^{-6}\ K^{-1}$, that is near the value of silicon ($3.5 \times 10^{-6}\ K^{-1}$), and a dielectric constant of 5.0 at 1 MHz [1], that is almost the half that of alumina (Al_2O_3) which is commonly used as the substrate for electric devices. These properties are very useful in substrates which are used for very large-scale integrated circuits. A sintered pellet which showed 96% relative density has been prepared previously by a sol–gel process using metal salts as raw materials [2], but it was necessary to sinter the pellet at 1300 °C for 12 h. A lower sintering temperature is more desirable for electric circuit use [3]. In the present work, B_2O_3 was added; this is used to reduce the crystallization temperature of cordierite in the conventional recrystallization method. There has been no report on the mechanism of low-temperature crystallization of cordierite using B_2O_3.

It is very important for the sol–gel process to control the amorphous structure before crystallization, although it is difficult to determine the structure using X-ray diffraction. Fyfe *et al.* [4] investigated the structural change of stoichiometric $Mg_2Al_4Si_5O_{18}$ glass heated at 1185 °C; from glass to indialite (α-$Mg_2Al_4Si_5O_{18}$), then to cordierite, measuring ^{29}Si and ^{27}Al magic angle spinning nuclear magnetic resonance (MAS NMR) spectra. They reported quantitatively the coordination structures of silicon and aluminium at each time during heating. To determine the role of B_2O_3 for low-temperature crystallization of $Mg_2Al_4Si_5O_{18}$, we measured ^{29}Si, ^{27}Al and ^{11}B MAS NMR spectra over the temperature range 100–1300 °C, and compared the results with those of thermogravimetric–differential thermal analysis (TG–DTA), X-ray diffraction (XRD), Fourier transform–infrared spectroscopy (FT–IR) and electron probe microanalysis (EPMA) measurements. The experiments clearly showed that the use of B_2O_3 in the sol–gel process produced indialite, which had the same electrical and mechanical properties as cordierite, on heating at 900 °C for 6 h. This is an interesting result because usually indialite is said to be stable above 1450 °C.

2. Experimental procedure

2.1. Preparation of the powder

$Al(NO_3)_3 \cdot 9H_2O$, $Mg(COOH)_2 \cdot 4H_2O$ and B_2O_3 were dissolved in a solvent, then mixed with tetraethoxysilane (TEOS) and stirred for 2 h at room temperature. The solution was poured into a thin alumina dish and dried at 80 °C for 24 h, then milled and heated at 600 °C for 4 h. The amorphous sample was milled again and heated at 900 °C for 4 h. Magnesium, aluminium and silicon were in the batch ratio 2:4:5, and B_2O_3 varied from 0–3.0 wt%. A mixture of ethanol and ethylene glycol was used as the solvent because of the good degree of crystallinity of $Mg_2Al_4Si_5O_{18}$ and wettability of the solution on alumina substrates. The volume ratio of the mixed solvent to TEOS was 5:1.

2.2. Preparation of the pellets for density, hardness and EPMA measurements

The amorphous powder heated at 600 °C for 4 h was uniaxially pressed at 190 MPa using an autograph (Shimazu model AG-10TA) to make a disc of 20 mm diameter and 5 mm thick. It was heated at 900 °C

0022–2461 © *1997 Chapman & Hall*

for 6 h (for EPMA, 700–900 °C, 4 h) and cooled in a furnace.

2.3. Preparation of the pellet for dielectric measurement

To make a thin pellet (1 mm in thickness, 13 mm dia.), a hand press and die (Shimazu Co.) was used instead of the autograph. The pressing conditions were: pre-press at 149 MPa, for 1 min; main press at 298 MPa, for 3 min. The pellets were heated at 900 °C for 6 h and cooled in the furnace.

2.4. Thermogravimetric and differential thermal analysis

The powder dried at 80 °C for 24 h was analysed by a TG–DTA measuring system (Rigaku model DTA–TG 8078). The heating rate was 10 °C min^{-1}.

2.5. Infrared absorption spectra (IR)

The powder heated at each temperature for 4 h after drying at 80 °C for 24 h was analysed using a Fourier transform–infrared absorption spectrophotometer (Shimazu model FT–IR 4200). The KBr method was used. The sample was dried at 120 °C for 24 h just prior to mixing with KBr powder.

2.6. X-ray diffraction (XRD)

The XRD spectra of the heated powder were measured using an X-ray diffractometer (Rigaku model CN4148) with a film attachment and a carbon monochromator. The CuK_α line was used and the incident angle, θ, was 5°.

2.7. MAS NMR spectra

Multinuclear MAS NMR spectra of the powder heated at each temperature for 4 h after drying at 80 °C for 24 h were measured using a high-resolution solid-state NMR spectrometer (JEOL model EX400). The measurement conditions are shown in Table I.

2.8. Electron probe microanalysis (EPMA)

After heating at 600 °C for 4 h, the pellets were heated at 700, 800 and 900 °C for 4 h, respectively. JEOL DATUM took EPMA measurements of these pellets (JEOL model JXA-8900). These samples were coated with a 15 nm thick carbon film by means of vacuum evaporation. The acceleration voltage and probe current of the electron beam were 15 kV and 2×10^{-8} A, respectively.

TABLE I MAS NMR measurement conditions

Nuclear	Temp. (°C)	Method	Standard (p.p.m.)
^{11}B	100–900	MASGHD	BPO_4 (− 3.60)
^{29}Si	100–600	CPMAS	TMS (− 34.00)
^{29}Si	700–1300	MASGHD	TMS (− 34.00)
^{27}Al	100–1300	MASGNN	$Al(NO_3)_3$ (0.00)

2.9. Density

The density of the pellet, ρ, was calculated using the weight in air, $W_{(\text{air})}$, and water, $W_{(\text{aqu})}$, following Equations 1 and 2

$$V = \frac{W_{(\text{air})} - W_{(\text{aqu})}}{\rho_{(\text{aqu})} - \rho_{(\text{air})}} \tag{1}$$

$$\rho = \frac{W_{(\text{air})}}{V} \tag{2}$$

where $\rho_{(\text{air})}$ is the density of air (≈ 0), $\rho_{(\text{aqu})}$ the density of water, and V the volume of the sample. We calculated the relative density as the ratio of the measured ρ to the theoretical density of completely sintered cordierite (2.5493 g cm^{-3}).

2.10. Vickers microhardness

Vickers hardness of the sample was measured using a microhardness meter (Akasi model MVK-EII), at a load weight of 500 g, a loading time of 10 s and ten points per sample.

2.11. Dielectric constant

Both bottom and top surfaces of the pellet were coated with gold by vacuum evaporation and the capacity, C, of the condenser was measured using an impedance gain phase analyser (YHP model 4194A). Relative dielectric constant, ε, was calculated from

$$\varepsilon = C\frac{d}{\varepsilon_0 S} \tag{3}$$

where d is the thickness of the pellet, S the surface area of the gold electrode, and ε_0 the dielectric constant of a vacuum (8.854×10^{-12} F m^{-1}).

3. Results

3.1. TG–DTA and FT–IR

Fig. 1 shows the result of TG–DTA measurement. The exothermic peak with a weight loss at around 400 °C suggests that organic matter is burned out by 600 °C.

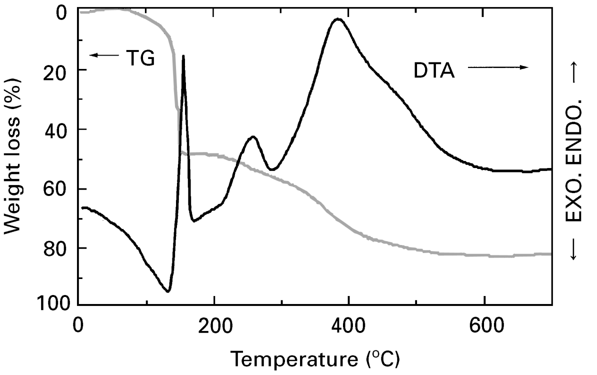

Figure 1 TG–DTA curves of a cordierite composition gel containing 1.5 wt % B_2O_3 and heated at 80 °C for 24 h.

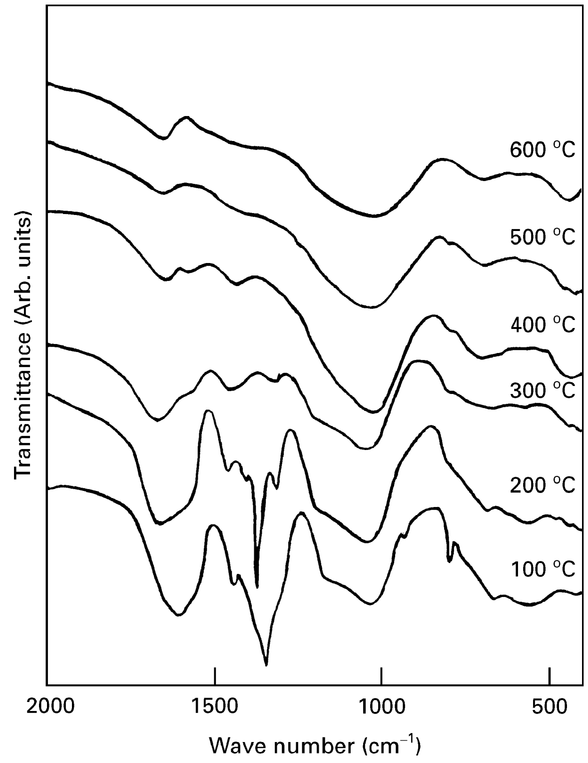

Figure 2 FT–IR spectra of the cordierite composition sample containing 2.1 wt % B_2O_3 and heated at each temperature for 4 h.

Fig. 2 shows the change of FT–IR spectra of the sample containing 2.1 wt % B_2O_3 with heating temperature. The peaks at 820 and 1380 cm^{-1} (nitrate ions) and 1400 cm^{-1} (alkyl group) decrease with increasing temperature and almost disappear by 600 °C. Without B_2O_3, these peaks disappear by 500 °C. The peak of =B–O–B= at 720 cm^{-1} cannot be seen, because of the small amount of B_2O_3 (5 wt %) and the existence of four-coordinated aluminium at 700 cm^{-1}. The peak of four-coordinated aluminium increases with increasing temperature, while the peak of six-coordinated aluminium at 590 cm^{-1} decreases [5].

3.2. XRD

Fig. 3 shows the change in the XRD patterns of the powder heated at 900 °C for 4 h with changing B_2O_3 content. Addition of 2.1 wt % B_2O_3 gives the largest peaks of α-$Mg_2Al_4Si_5O_{18}$ and the smallest peaks of μ-$Mg_2Al_4Si_5O_{18}$ and impurities like mullite ($Al_6Si_2O_{13}$) and spinel ($MgAl_2O_4$).

Fig. 4 shows the change in the XRD patterns of the powder containing 2.1 wt % B_2O_3 with heating temperature. α-phase and the impurities begin to crystallize between 800 and 850 °C. At 900 °C the peaks of α-phase show a maximum intensity and the others almost disappear.

Fig. 5 shows the change in the XRD patterns of the powder without B_2O_3 with heating temperature. Crystallization occurs between 800 and 900 °C as in Fig. 4. However, in this case, μ-phase appears with β-phase at 700 °C. At 1000 °C, mullite also appears and exists up to 1100 °C with the μ-phase. Above 1100 °C, μ-phase and mullite disappear and β-phase rapidly increases. At 1200 °C, β-phase shows a maximum intensity. It is said that β-phase develops from μ-phase when the homogeneity of the amorphous state is low [6, 7].

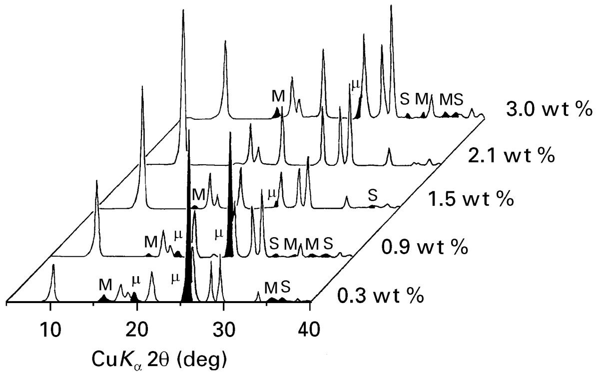

Figure 3 Change of XRD pattern of the powder heated at 900 °C for 4 h with changing B_2O_3 content. μ, μ-phase; M, mullite; S, spinel.

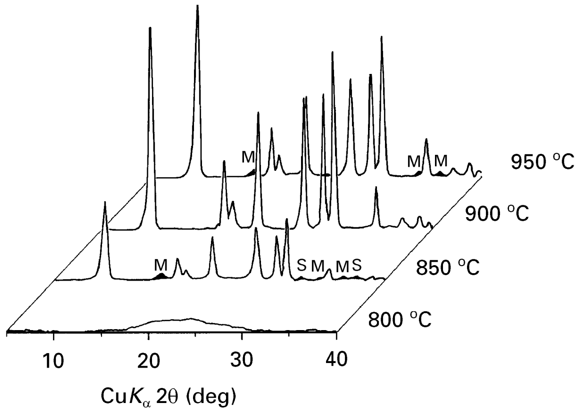

Figure 4 XRD patterns of the powder containing 2.1 wt % B_2O_3 and heated at each temperature for 4 h. M, mullite; S, spinel.

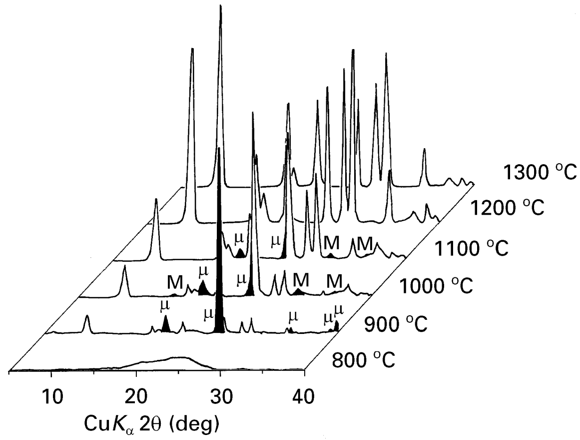

Figure 5 XRD patterns of the powder without B_2O_3 heated at each temperature for 4 h. μ, μ-phase; M, mullite.

3.3. NMR

Fig. 6 shows the change of ^{29}Si NMR spectra of the powder heated for 4 h with heating temperature between 100 and 500 °C for B_2O_3 contents of (a) 0 and (b) 2.1 wt %. Both spectra appear to be almost the same, although there are slight differences between

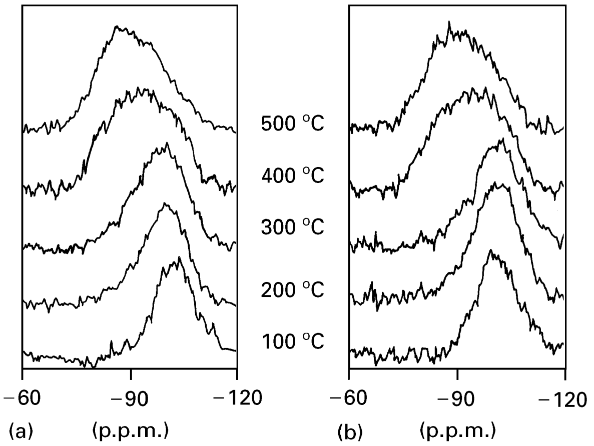

Figure 6 ^{29}Si NMR spectra of the powder heated at each temperature (100–500 °C) for 4 h. B_2O_3 content: (a) 0, (b) 2.1 wt %.

them. In Fig. 6b the wide peak does not change its position between 100 and 300 °C, but begins to shift to the higher frequency side above 300 °C. In Fig. 6a, the wide peak gradually shifts to the higher frequency side with increasing temperature between 100 and 300 °C. Those shifts suggest an increase in the number of aluminium atoms coordinated with silicon ($Q^4(n\text{Al})$, $n = 1, 2, 3, 4$ [8, 9]). Above 300 °C Fig. 6a shows the same tendency as Fig. 6b. In other words, n rapidly increases with increasing temperature between 300 and 500 °C in both cases.

Fig. 7 shows the change of ^{29}Si NMR spectra with heating temperature between 600 and 900 °C. In this temperature range, some clear differences between (a) and (b) can be seen. The profiles at 600 °C are almost the same as those at 500 °C in both cases. But at 700 °C, the peak becomes broader and shifts to the lower frequency side in (b) than that in (a). In other words, the Si–O–Al bonds are broken by boron. There are very small $Q^4(4\text{Al})$ peaks (≈ -79 and ≈ -95 p.p.m.) in (b) though they are clearly seen in (a) at 900 °C. The peak profile in (b) at 900 °C is almost the same as that of α-phase [4], but the peak profile in (a) is broader than that in (b). Thus there are some coordination structures involving μ- and β-phases in the case of (a). The difference in the measuring method, cross polarization-MAS (CPMAS) (below 600 °C) and gated high power decoupling-MAS (MASGHD) (above 700 °C), has no essential effect on the NMR profile, because there is little change between 600 and 700 °C in (a) and organic matter has already burned out by 600 °C.

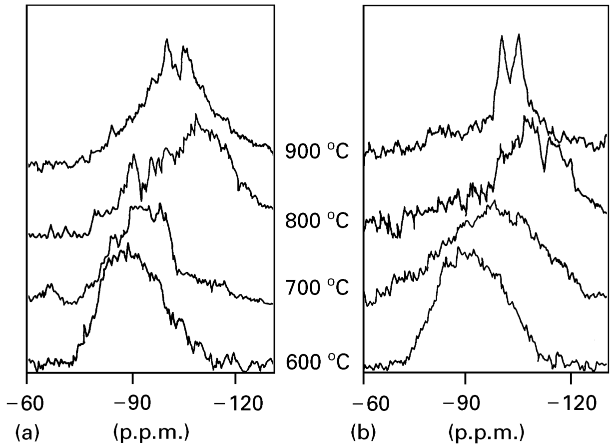

Figure 7 ^{29}Si NMR spectra of the powder heated at each temperature (600–900 °C) for 4 h. B_2O_3 content: (a) 0, (b) 2.1 wt %.

Fig. 8 shows the change of ^{27}Al NMR spectra [10, 11] with heating temperature between 100 and 900 °C. In contrast with ^{29}Si NMR spectra, there are significant differences between (a) and (b) below 600 °C and at 900 °C, although they show a slight difference between 700 and 800 °C. In the case of (b), the peaks shift to the higher frequency side between 300 and 400 °C, and the peak of six-coordinated aluminium (≈ 5 p.p.m.) does not disappear until 900 °C. On the other hand, the peaks begin to shift to the higher frequency side at 100 °C and the peak of six-coordinated aluminium disappears at 600 °C in the case of (a). The peak profile of (b) changes more significantly than that of (a) between 800 and 900 °C. The peak profile of (b) at 900 °C is almost the same as that of α-phase [4].

Fig. 9 shows the change of ^{11}B NMR spectra with heating temperature for a B_2O_3 content of 2.1 wt %. Four-coordinated boron (≈ 0 p.p.m.) increases rapidly while three-coordinated boron (≈ 12 p.p.m.) [12, 13] decreases with increasing temperature between 300 and 400 °C. The peak profile becomes broader and three-coordinated boron increases with decreasing four-coordinated boron between 600 and 700 °C. At 900 °C four-coordinated boron increases again and the half-width of the peak decreases.

Fig. 10 shows the changes of ^{29}Si and ^{27}Al NMR spectra with varying B_2O_3 content from 0–3.0 wt %. Samples were heated at 900 °C for 4 h. The peak intensity of four-coordinated aluminium (≈ 70 p.p.m.) shows its maximum at 2.1 wt % B_2O_3 content. At the same content, ^{29}Si NMR shows almost the same shape as the α-phase.

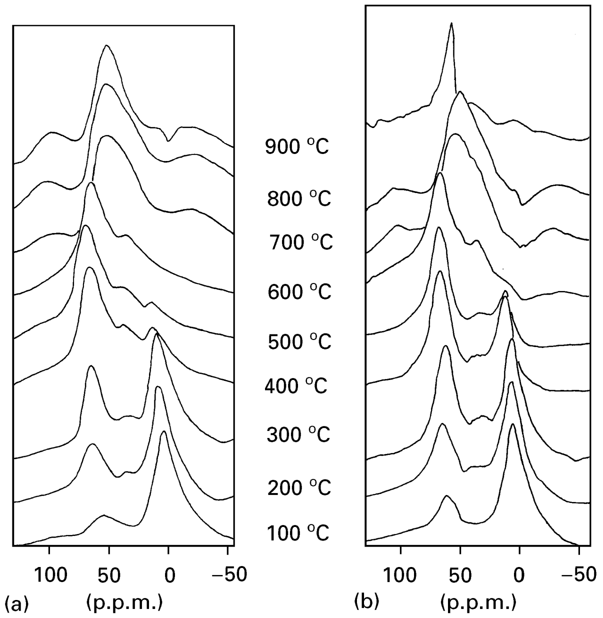

Figure 8 ^{27}Al NMR spectra of the powder heated at each temperature for 4 h. B_2O_3 content: (a) 0, (b) 2.1 wt %.

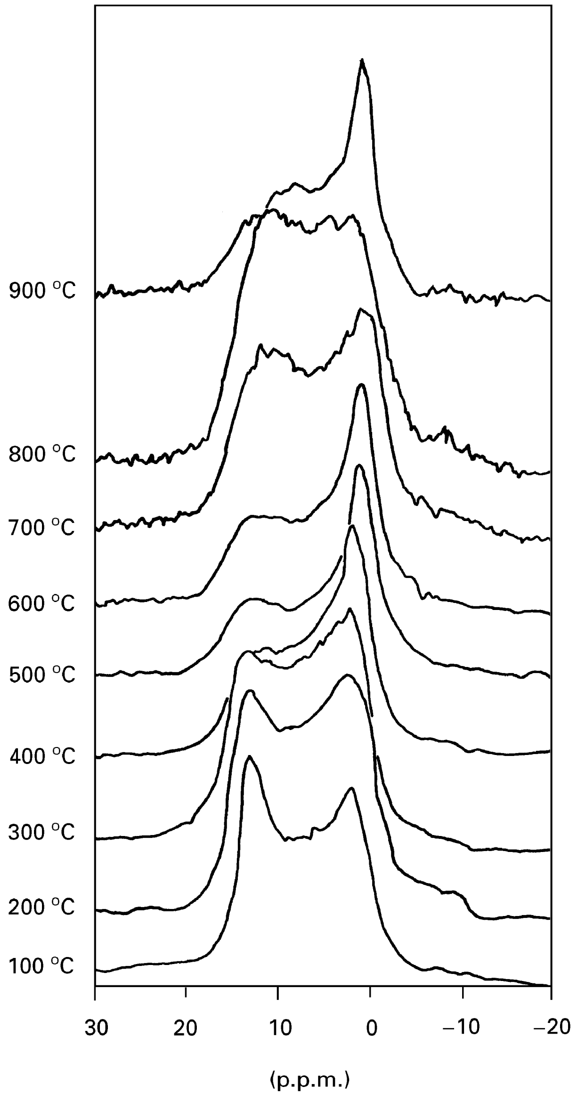

Figure 9 ^{11}B NMR spectra of the powder including 2.1 wt % B_2O_3 and heated at each temperature for 4 h.

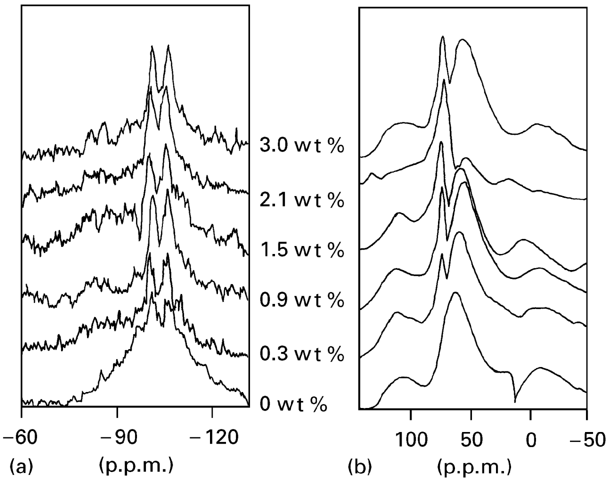

Figure 10 Changes of (a)^{29}Si and (b) ^{27}Al NMR spectra of the sample heated at 900 °C for 4 h with varying B_2O_3 content.

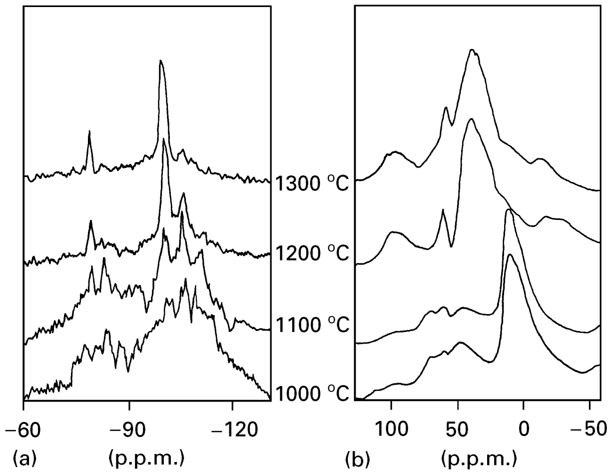

Figure 11 (a)^{29}Si and (b)^{27}Al NMR spectra of the sample without B_2O_3 heated at each temperature for 4 h.

Fig. 11 shows the change of ^{29}Si and ^{27}Al NMR spectra of the sample without B_2O_3 with heating temperature between 1000 and 1300 °C. Samples were heated for 4 h at each temperature. Above 1100 °C certain structural change occur significantly. Here, μ-phase and mullite are transformed to β-phase as shown in the results of XRD measurements. Silicon atoms at T^1 and T^2 sites (≈ -79 and ≈ -100 p.p.m., respectively) are four- and three-coordinated with aluminium atoms [4] at 1300 °C, respectively. Comparing both profiles of ^{29}Si and ^{27}Al NMR spectra at 1300 °C with the reported spectra [4], it is concluded that the sample is mainly composed of β-phase with a small amount of α-phase. To obtain the same spectra, the glass recrystallization method [4] requires a further heating at 1185 °C for about 100 h.

3.4. SEM

SEM images of the pellets that were heated at 800 °C for 4 h were taken by JEOL DATUM during the EPMA measurements. B_2O_3 contents of the pellets were (a) 0 and (b) 2.1 wt %, respectively. In (b) there were many round dips. It suggested that partial melting occurred by a reaction between silicon and boron [14]. These dips were also seen when the sample containing 2.1 wt % B_2O_3 was heated at 700 °C. However, when the sample was heated at 900 °C, no round dips were found.

3.5. EPMA

Table II shows the EPMA results of a sample heated at 900 °C for 4 h. The composition ratio of magnesium to aluminium was stoichiometric, though silicon was detected in amounts about 7% larger than the stoichiometric value. The measured B_2O_3 content was larger than that of the batch (2.1 wt %). It is well known that the quantitative analysis of a light atom such as boron is very difficult by means of EPMA.

3.6. Density, Vickers hardness and dielectric constant

Table III shows the density, Vickers hardness and dielectric constant results. When heated at 900 °C for 6 h, the pellets containing 2.1 wt % B_2O_3 showed

TABLE II EPMA results of a sample heated at 900 °C for 4 h

	B_2O_3	MgO	Al_2O_3	SiO_2	Total	
(wt %)	3.5	12.9	32.52	51.3	100.2	
	B	Mg	Al	Si	Total	Total O
Atomic ratio	0.593	1.89	3.78	5.06	11.3	18.5

TABLE III Density, Vickers hardness and relative dielectric constant of the samples heated at each temperature for 6 h

	Sample		
	2.1 wt % B_2O_3, 900 °C	0 wt % B_2O_3, 1200 °C	Reference
Relative density (%)	91.4	93.3	100 (=2.55 g cm^3)
Vickers hardness	1080	1030	
Relative dielectric constant	5.0	5.0	5.0 (cordierite)

more than 90% relative density, 1080 Vickers hardness and a relative dielectric constant of 5.0, which was the same as the reported value.

4. Discussion

From these experimental results, we can consider the crystallization processes of $Mg_2Al_4Si_5O_{18}$ in both systems with and without B_2O_3. A comparison is made in Tables IV and V. Without B_2O_3, it can be seen that μ-phase first crystallizes just above 800 °C and transforms to β-phase at about 1100 °C. With 2.1 wt % B_2O_3, almost single α-phase was prepared at 900 °C directly from the amorphous state. By disturbing the formation of the Si–O–Al network below 300 °C, boron retains the high homogeneity of the system before crystallization. The melting caused by boron between 700 and 800°C results in a high homogeneity and fluidity of the system. Thus α-phase crystallizes easily between 800 and 850 °C. ^{29}Si and ^{27}Al NMR spectra of the sample heated at 900 °C for 4 h were almost the same as those of the α-phase. The ^{11}B NMR spectrum showed a sharp four-coordinated peak at that temperature. These results suggest that boron is segregated at the grain boundary of the α-phase at 900 °C. The small amount of boron at the grain boundary is considered to allow the α-phase to continue to grow stably at 900 °C, although usually α-phase is stable only above 1450 °C [4].

TABLE IV Crystallization process of $Mg_2Al_4Si_5O_{18}$ without B_2O_3

Temperature (°C)	State
~300	Al–O–Si bonds forms partially (may be only at the surface of SiO_2 colloid particles).
300~	Al–O–Si bonds increase. → Low homogeneity.
~500	Organic matter disappears.
800–900	μ and β-phases begin to crystallize.
900–1100	Small amount of mullite also crystallizes.
1100~	μ-phase and mullite are transformed to β-phase. β-phase will increase upto 1450 °C because the phase is stable between 1050 and 1450 °C [4].

TABLE V Crystallization process of $Mg_2Al_4Si_5O_{18}$ with 2.1 wt% B_2O_3

Temperature (°C)	State
~300	Al is coordinated by B_2O_3. Al cannot bond well with Si–O–Si colloid particles.
300~	Al–O–Si bond forms. B (four-coordinated) condenses around Al–O–Si particles.
~600	Organic matter disappears.
700–800	The condensed B reacts with Si in the Al–O–Si particle. This results in the melting of the system. → High homogeneity and fluidity.
800–850	α-phase begins to crystallize with small amounts of mullite and spinel.
850–900	Mullite and spinel are transformed to α-phase.

5. Conclusions

By comparing the results of TG–DTA, XRD, FT–IR, EPMA with ^{29}Si, ^{27}Al and ^{11}B MAS NMR spectra, the following results were obtained.

1. When 2.1 wt % B_2O_3 was added, powder and pellets composed mainly of indialite (α-$Mg_2Al_4Si_5O_{18}$) could be prepared by heating at 900 °C for 6 h by a sol–gel process using metal salts as raw materials. This is a quite interesting result, because usually α-$Mg_2Al_4Si_5O_{18}$ is said to be stable above 1450 °C.

2. The relative density, Vickers hardness and relative dielectric constant at 1 MHz of the pellet were 91.4%, 1080 and 5.0, respectively.

3. Boron disturbs the formation of the Si–O–Al network below 300 °C and breaks the network between 700 and 800 °C. The high homogeneity and fluidity on melting help α-$Mg_2Al_4Si_5O_{18}$ to crystallize between 800 and 850 °C.

References

1. “Dictionary of Fine Ceramics” edited by Committee of Dictionary (Gihodo, Tokyo, 1987) (in Japanese).
2. N. KIKUCHI, T. SEI, T. TSUCHIYA, S. HAYASHI and K. HAYAMIZU, *J. Ceram. Soc. Jpn* **101** (1993) 824.
3. M. OKUYAMA, T. FUKUI and C. SAKURAI, *J. Mater. Res. Soc.* **7** (1992) 2281.
4. C. A. FYFE, G. C. GOBBI and A. PUTNIS, *J. Amer. Chem. Soc.* **108** (1986) 3218.

5. S. H. KWON and S. J. CHUNG, *Phys. Chem. Glasses* **28** (1987) 28.
6. U. SELVARA, J. S. KOMARNANI and R. ROY, *J. Amer. Ceram. Soc.* **73** (1990) 3663.
7. A. D. IRWIN, J. S. HOLMGREN and J. JONAS, *J. Non-Cryst. Solids* **101** (1988) 249.
8. C. I. MERZBACHER, K. J. MCGRATH and P. L. HIGBY, *ibid.* **136** (1991) 249.
9. S. H. RISBUD, R. J. KIRKPATRIC, A. P. TAGLIALAVORE and B. MONTEZ, *J. Amer. Ceram. Soc.* **70** (1987) C-10.
10. G. ENGELHARDT and D. MECHEL "High-Resolution Solid-State NMR of Silica and Zeolites" (Wiley, New York, 1987) p. 143.
11. C. A. FYFE, G. C. GOBBI, J. S. HARTMAN, J. KLLNOWSKI and J. M. THOMAS, *J. Phys. Chem.* **86** (1982) 1247.
12. S. HAYASHI and S.NAKATA, "Solid-state NMR of Materials by Chart" (Kodansha, Tokyo, 1993).
13. S. KOMARNENI, C. A. FYFE, G. J. KENNEDY and H. STROBL, *J. Amer. Ceram. Soc.* **69** (1986) C45.
14. T. J. ROCKETT and W. R. FOSTER, *ibid.* **48** (1965) 78.

Received 8 December 1995
and accepted 7 January 1996